FUNDAMENTALS & APPLICATIONS FOR NON-DESTRUCTIVE TESTING

This completely updated 2nd edition of Eddy Current Testing Technology meets and exceeds ISO9712, CGSB, ASNT, and CSWIP theoretical requirements for Level 1 & 2 certification. Several new topics have been added that enable individuals to effectively apply Eddy Current Testing techniques to achieve a quality inspection; this includes:

- **Theoretical Concepts:** mathematical formulas supported by worked examples; new graphs and tables are utilized to help illustrate theory concepts.
- **Acquisition Techniques:** a wide collection of real-life inspection applications are discussed with tips and guidelines.
- **Analysis Methodologies:** signal pattern recognition, sizing, and flaw positioning methods are explained in detail with examples.
- **Ferromagnetic Inspections:** a completely new topic that outlines data acquisition and analysis.
- **Technical Justification:** concepts and principles for conducting case studies and qualifications.
- **Inspection Procedures:** awareness and guidelines for preparing effective procedures.

I wrote this book with the intent of having a continual flow between topics. I hope this book will serve as an excellent resource for learning Eddy Current Testing and preparing for a certification exam.

Michael Wright

TECHNOLOGY
EDUCATION
CONFIDENCE
CERTIFICATION
EXPERTISE

ISBN 978-0-9917095-6-4

9 780991 709564 >

www.eclipsescientific.com

ECLIPSE SCIENTIFIC

EDDY CURRENT TESTING TECHNOLOGY

2nd Edition

EDDY CURRENT TESTING TECHNOLOGY

2nd Edition

ECLIPSE SCIENTIFIC

TABLE OF CONTENTS

CHAPTER (27): FERROMAGNETIC INSPECTION GUIDELINES

27.1 INTRODUCTION

The relative permeability of ferromagnetic material is high, so the depth of penetration for an eddy current test is very low. With typical mild steel, at 5 kHz the standard depth of penetration is around 0.25mm. With such a shallow depth of penetration, unless a defect has been demonstrated to be detectable, defects should be limited to surface-breaking defects only.

The inspection of ferromagnetic materials for surface-breaking indications is not only possible, but is a fairly easy process that usually yields good results. With some inspections, depth sizing with confidence is also possible.

27.2 LOCUS CURVES

Many Locus curves are called Loci. Loci with permeability greater than one move vertically above 1 in the impedance plane. These curves are very large compared to the non-magnetic permeability loci. As the permeability increases the operating point moves higher in the impedance plane.

Figure 27-1 shows a locus curve with a permeability that varies from 1 to 10000. This was generated at 50kHz using Teddy software.

Teddy software is a freeware impedance calculating utility by Dr. Theodoros P. Theodoulidis.

Region D shows the impedance plane location for the operating point having permeability from 1 to 10. Region C shows permeability from 10 to 100. Region B shows permeability from 100 to 1000 and region A shows permeability from 1000 to 10000.

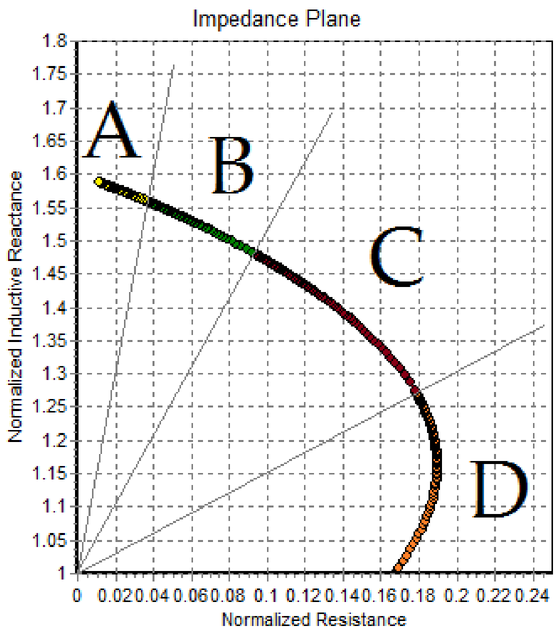

Figure 27-1 Locus curve showing a relative permeability of 1 through 10000

Carbon steel would only occupy locus points in region B since it has a permeability of 100 to 1000. Many of the 400 series stainless steels would be in region D. Region C would have nickel steels and some alloy steels. Region A would be Permalloy and some cobalt steels. The region that would be above A would be Mu-metal and ferrite itself.

Each probe type has different shaped loci. For example, transmit-receive loci would not have the same shape as an absolute loci. Also, probe characteristics of each probe type would have different loci.

Figure 27-2 shows 5 different loci created from a permeability of 1 to 1000. Loci A to E were generated using a 4 mm to 8 mm diameter absolute probe respectively using a 1 mm step.

Absolute and differential probes can be used very successfully on carbon steel material; but transmit-receive, orthogonal, and other custom sensors are more commonly used to help minimize noise levels.

With magnetic material there is additional noise from permeability variations, hysteresis effects, and an increase in lift-off sensitivity.

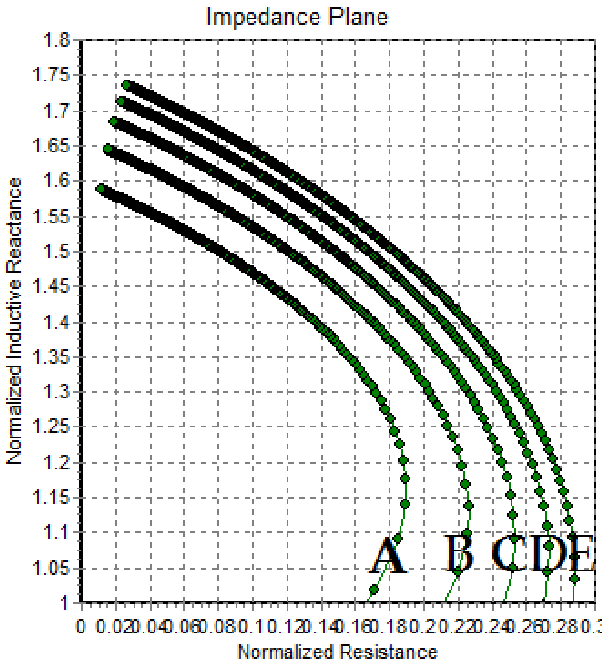

Figure 27-2 Locus curve generated from different probe diameters

The lift-off sensitivity is increased since the excitation signal energy does not penetrate into the test material easily. This surface concentration, or increased skin effect, yields a higher sensitivity to surface conditions. With most tests, the increase in sensitivity creates a great increase in noise.

27.3 MATERIAL SORTING

Sorting of ferromagnetic material can be done with various levels of success. All probes and techniques must be validated using performance demonstrations or with technical justifications. If the material noise levels are low, the sorting of material types and properties will be successful. If the noise levels are high, sorting can become a statistical process and the number of sorting bins will likely be reduced.

Figure 27-3 shows an impedance diagram of different carbon steels generated using an absolute probe.

Ferrite can be seen going straight upwards. A is a sample of 1045 CS, B is 1018CS, C is 4140, D is 4140 annealed, E is D2, and F is A2, G is tungsten, and H is Inconel.

This permeability locus fits the theoretically calculated locus very closely. With this test situation material, A would easily be sorted from the other materials. Materials E and F trace nearly identical lift-off curves and have final operating points that are very close. In this test situation these two materials could not be sorted.

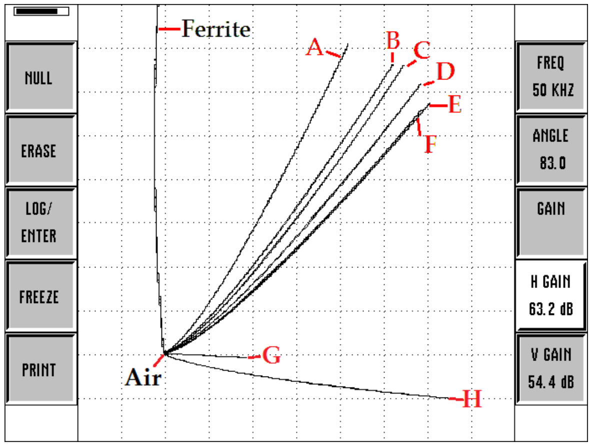

Figure 27-3 Absolute impedance plane showing different carbon steel grades

27.4 NOISE SIGNALS

27.4.1 LIFT-OFF VARIATIONS

Lift-off variations from magnetic material are virtually the same as non-magnetic material. The main difference being the vertical nature of the magnetic impedance signals.

Permeability changes are extremely nonlinear while lift-off variations tend to remain similar between different permeability levels.

This yields a test situation where material with a lower permeability will see larger variations in permeability changes. Material with a higher permeability will have very little operating point motion due to permeability changes as compared to larger operating point changes with small lift-off.

Figure 27-4 shows a Teddy model with permeability in the carbon steel range (100 to 1000). Each blue line shows lift-off steps of 0.25 mm. Each blue lift-off curve was generated with a step of 100µ.

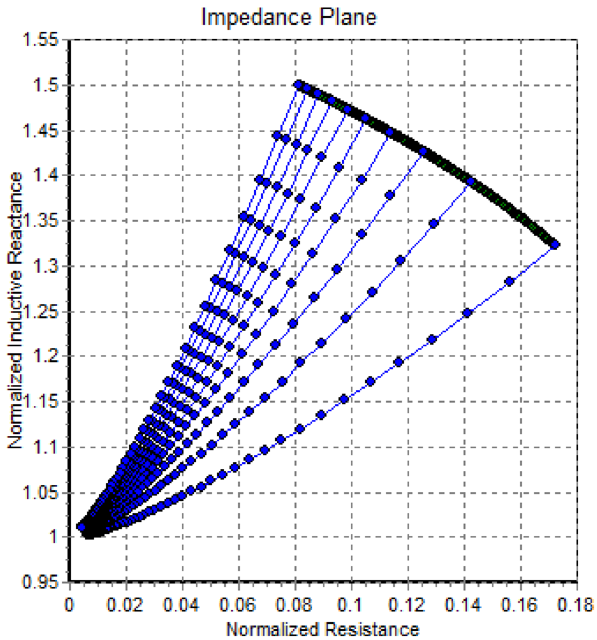

Figure 27-4 Absolute probe lift-off response

27.4.2 PERMEABILITY VARIATIONS

The carbon content and the existence of ferrite phase greatly influence the magnetic permeability of a ferromagnetic material. It also depends on the magnetic field strength to which the material is submitted. The magnetic field applied by an eddy current sensor is generated by applying AC to the sensor. This creates a sinusoidal-based magnetic field or an alternating magnetic field. The strength of the applied field is relatively low, but even with a weak magnetic field applied to a ferromagnetic material, the material will respond with a small hysteresis response. Remember, the permeability is represented by the following:

$$B = \mu H \tag{27.1}$$

Small variations in H produce either a small variation in B and/or in μ. Any variation from μ will cause impedance variations along the permeability locus curve. As a scan is performed, the permeability variations will trace a small wobble in the signal, making the variations very obvious.

Variations in chemistry or crystalline structure can create localized permeability variations that are generally larger than those created by the probe.

Figure 27-5 shows the impedance plane with a typical inspection orientation. Lift-off is set up moving horizontal and to the left. This image was optimized for material C. Materials A and D are tilted out of calibration since the lift-off is not quite flat.

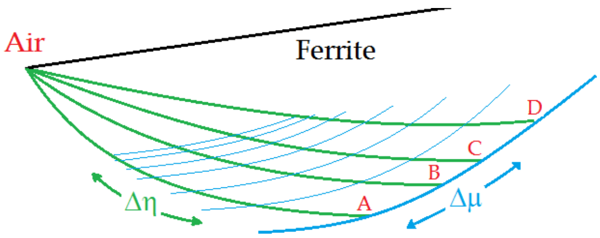

Figure 27-5 Absolute probe impedance plane showing signal variations

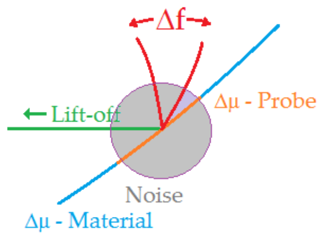

Figure 27-6 Absolute sensor ferromagnetic flaw plane

Figure 27-6 shows a zoomed in or screen view of inspection spot C. This illustrates the flaw plane for an absolute ferromagnetic crack inspection. The typical or average noise level is contained in the grey circular region. This average noise level contains the permeability variations generated from the probe's applied magnetic field. Lift-off and the air path are very close and usually cannot be separated. A signal from a crack is typically towards the ferrite response. This is due to a crack having magnetic flux leakage. The magnetic flux leakage will influence the probe response and create a vector combination towards air, but also towards ferrite. If a test probe does not interact or sense the flux leakage, the crack will create a probe response showing a decrease in permeability.

This is one of many reasons that all probes should be tested with performance demonstrations and/or technical justifications.

Figure 27-7 shows a scan of 1045 carbon steel calibration standard with several EDM notches. This example signal has the initial transition from lift-off moving horizontally to the left.

The variations from permeability can easily be seen to move in a linear wobble. They are tilted almost 135° from lift-off.

Even with the fairly consistent linear range of permeability variations, depth sizing becomes complicated. Using any type of measurement method other than a manual measurement will produce very inaccurate results. Manual measurement can be used with a higher degree of accuracy. If the permeability variations are consistent and large, depth sizing might not be achievable with any level of confidence.

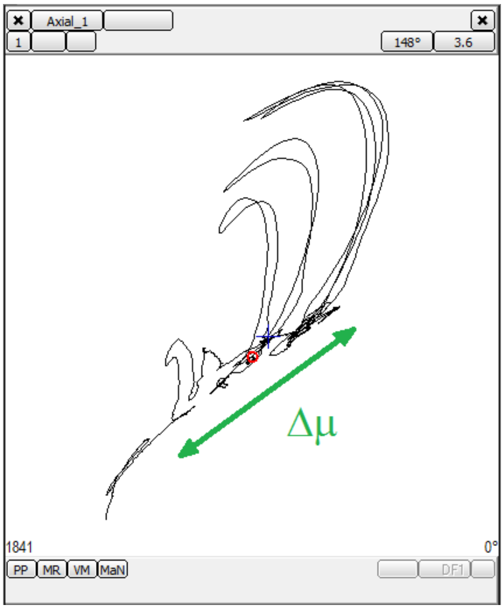

Figure 27-7 G3 T/R sensor permeability variation

27.4.3 MATERIAL VARIATIONS

Grain size, chemical composition, permeability, hardness, and residual magnetism can all influence the flow of eddy currents. Any material variation that alters the flow of eddy currents will be seen in the movement or final position of the operating point. Common inspection variables include:

- Heat effects: fire damage, localized welding, heat treatments, grinding marks
- Density variations: dents, variations in material hardness and chemical variations
- Defect detection: surface-breaking crack detection and corrosion detection
- Material sorting: hardness, permeability
- Conductive coating characterization: thickness (non-ferromagnetic coating) and integrity
- Non-conductive coating characterization: thickness measurements

27.5 CRACK DETECTION

27.5.1 ABSOLUTE SENSOR

The absolute sensor can be used for crack detection and crack depth sizing within the limitations outlined with a performance demonstration or technical justification. The main disadvantage is the high sensitivity to surface conditions and lift-off. If the test surface is very uniform and smooth, the absolute sensor can produce very reliable results.

Figure 27-8 shows an example inspection of a very smooth carbon steel test material. This example shows the average noise levels circled in red, lift-off response, and the signal response from 3 EDM notches. EDM notches 1 to 3 are 1 mm, 2 mm, and 3 mm respectively.

This example shows a probe response where defect detection is possible, but depth sizing with any level of accuracy is not possible. This inspection is set up as a pass/fail inspection.

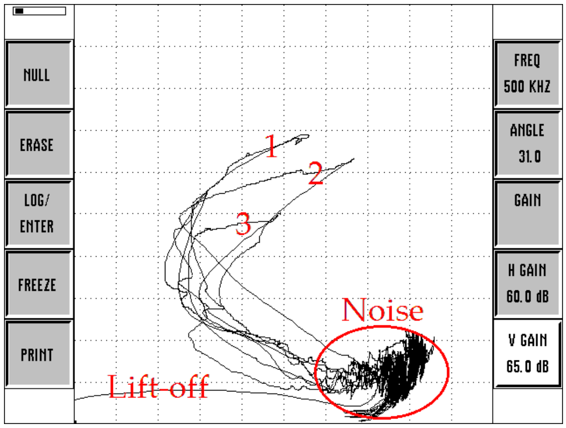

Figure 27-8 Absolute sensor defect response

27.5.2 DIFFERENTIAL SENSOR

The differential sensor can be used for crack detection and crack depth sizing within limitations outlined with a performance demonstration or technical justification. The differential sensor is normally the first sensor to test with, due to the lower sensitivity to lift-off and surface condition variations.

Figure 27-9 shows an example inspection using a very sensitive differential probe. This signal example shows the average noise level, lift-off response, and an EDM response. This EDM is 0.1 mm wide, 0.5 mm deep and 1.0 mm long.

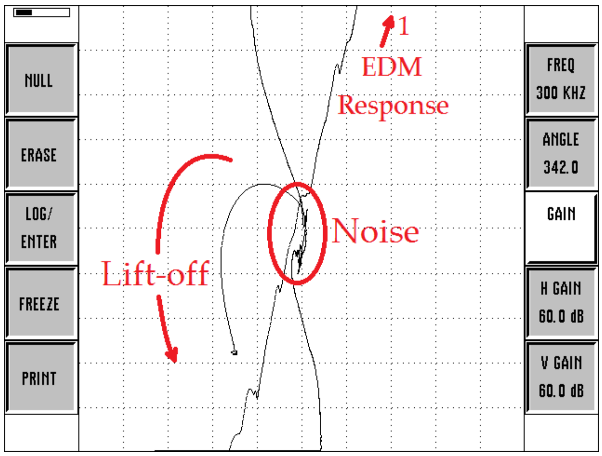

Figure 27-9 Differential sensor defect response

This inspection example also yielded a test that worked well for defect detection, but depth sizing was not possible. Although depth sizing was not possible with the use of encoders, length sizing became possible and accurate.

27.5.3 T/R SENSOR & ORTHOGONAL SENSOR

Transmit-receive sensors can be used with great success on ferromagnetic material when inspecting for surface-breaking indications. As the coil diameter and coil spacing is reduced the probe noise response increases. Transmit-receive sensor selection is a compromise between the noise level and the minimum detectable defect size. As the coil set is reduced, the sensitivity for smaller defects increases and the level of noise also increases. There is an optimal sensor size and layout for each target size.

The T/R sensor can easily be used for weld inspections. The T/R sensor is also ideal for array technology where several T/R probes are readily available for ferromagnetic weld inspection. With a T/R array, median filtering is commonly used to help smooth and clean up noise levels. If any filtering is used a proper technical justification should be performed to ensure the filtering process does not filter out the indications of interest.

Orthogonal sensors have very low noise levels from surface variations and are ideal sensors for weld inspection. The variations from the weld geometry, such as a weld cap, will add very little noise to the signal. Orthogonal probes also have the added benefit of being directionally sensitive to linear indications. This helps inspect a weld for longitudinal and transverse defects in a single pass.

27.6 CRACK DEPTH SIZING

The following depth sizing examples/demonstrations were generated using the calibration standard shown in Figure 27-10. This standard is made from 1018 carbon steel. The calibration curves generated from this standard will only apply to other electrically similar 1018 carbon steel test materials. With the following examples the depth sizing works well, but that does not mean that the depth sizing will work with all probes. Also, the depth sizing works in these examples using 1018 carbon steel, but different materials have to be tested to verify accuracy levels and what level will work.

This calibration sample has EDMs notches with 1.5 mm, 1.25 mm, 1.0 mm, 0.75 mm, & 0.5 mm depths. The thickness of a calibration standard does not really factor into an inspection since all ferromagnetic inspections will be limited to surface-breaking indications only.

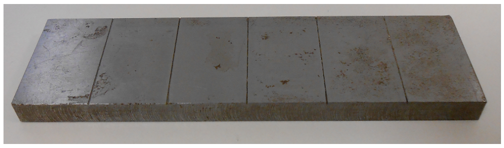

Figure 27-10 1018 CS depth sizing calibration standard

27.6.1 ABSOLUTE SENSOR DEPTH SIZING

With this example a single coil absolute sensor 8 mm in diameter was used. It was operated at 50 kHz. 50 kHz and 5 kHz are very common frequencies used when testing ferromagnetic material. This is due only to the reduced levels of noise. Low frequency does not generate deep penetration with magnetic material, so lowering the frequency does not normally yield many benefits. Lower frequency is used only if it can be demonstrated to produce benefits for the inspection.

Figure 27-11 to Figure 27-15 show the probe response of 0.5 mm to 1.5 mm deep notches on the calibration standard. Figure 27-16 shows the resulting magnitude calibration curve. This curve also produced a high accuracy level.

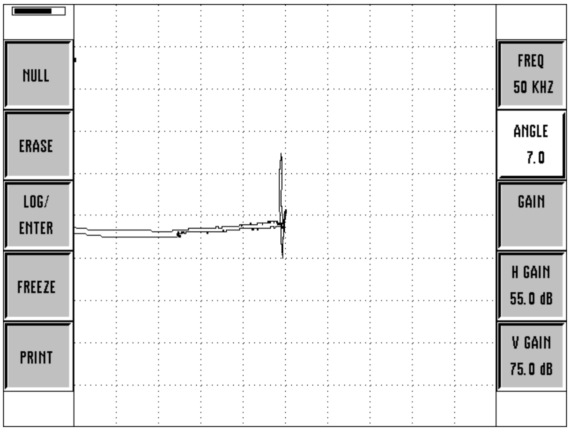

Figure 27-11 0.5 mm deep absolute signal

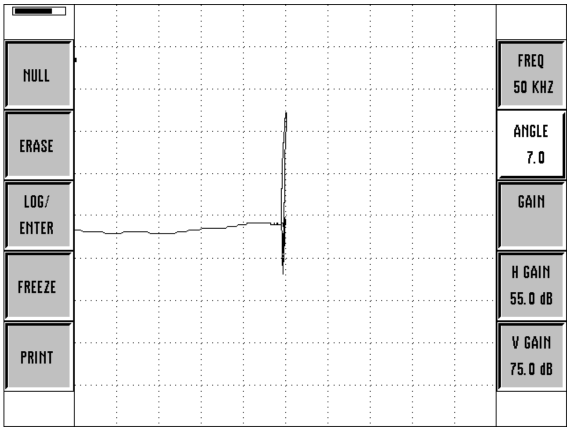

Figure 27-12 0.75 mm deep absolute signal

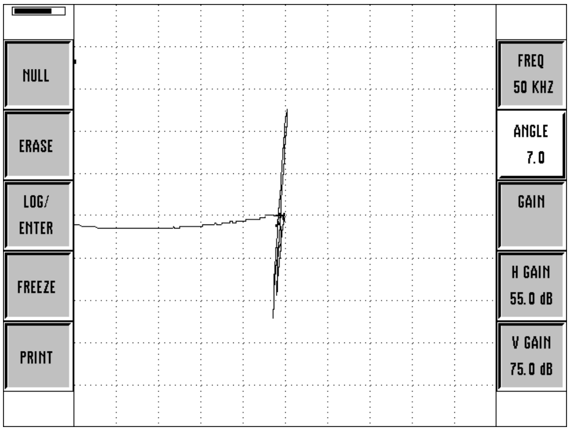

Figure 27-13 1.0 mm deep absolute signal

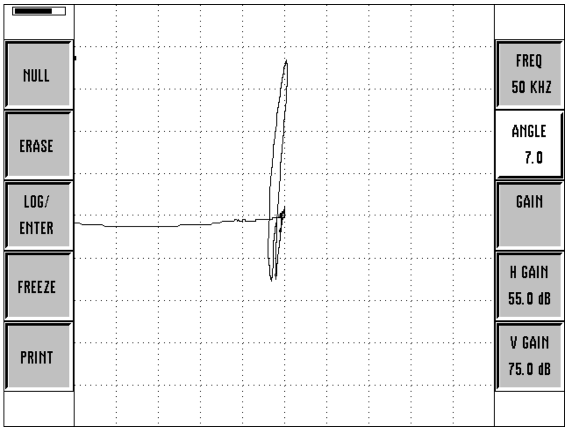

Figure 27-14 1.25 mm deep absolute signal

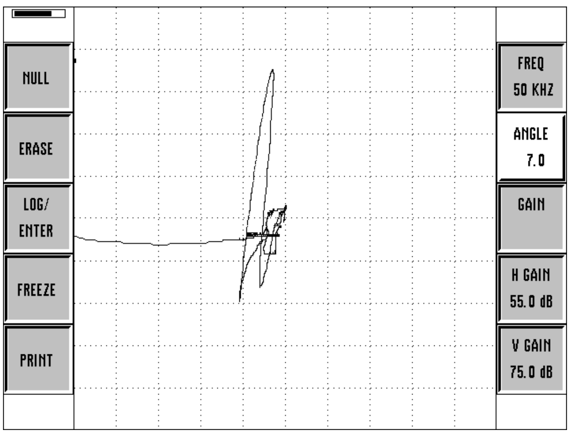

Figure 27-15 1.5 mm deep absolute signal

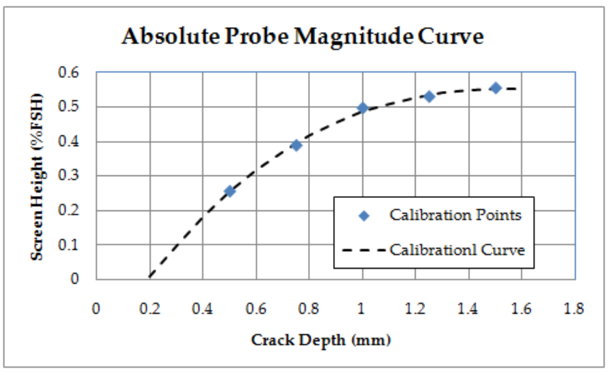

Figure 27-16 0.5 mm deep absolute signal

27.6.2 TRANSMIT-RECEIVE SENSOR DEPTH SIZING

With this example, a G3 mode, transmit-receive sensor with 3 mm coils and 10 mm coil spacing was used. It was operated at 150 kHz. This probe is designed to work between 50 kHz and 500 kHz when testing ferromagnetic material.

Figure 27-17 shows the probe response to the 0.5 mm to 1.5 mm deep notch on the calibration standard. Figure 27-18 shows the resulting magnitude calibration curve. This curve also produced a high accuracy level for regions with low permeability variations. This T/R probe was qualified to find indications that are 1.5 mm in length.

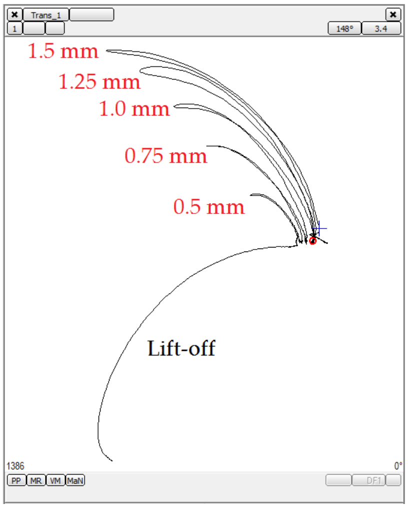

Figure 27-17 G3 T/R probe response

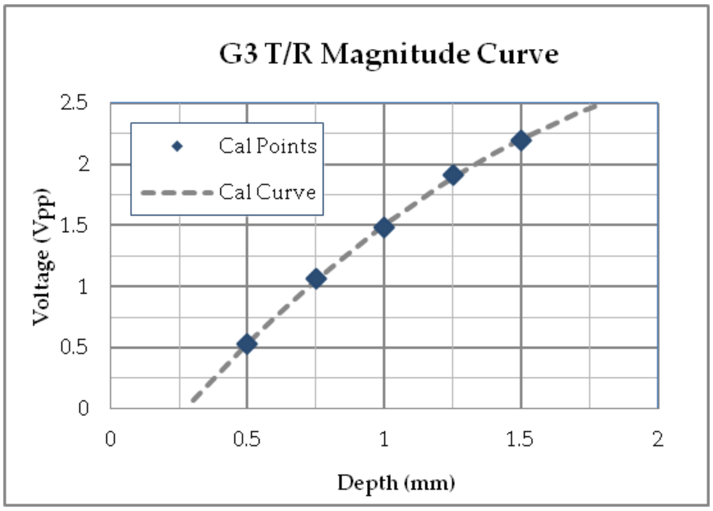

Figure 27-18 G3 T/R sensor magnitude curve

With this example, a phase curve could not be constructed since the defects responded with nearly identical phase.

27.6.3 ORTHOGONAL SENSOR DEPTH SIZING

With this example, a standard bridge orthogonal sensor 8 mm in diameter was used. It was operated at 500 kHz. These sensors have very little noise or sensitivity to surface variations and can be operated at much higher frequencies for surface-breaking crack detection. The higher frequency reduces the noise from unwanted material variations.

Figure 27-19 shows the orthogonal sensor response to the targets in the calibration standard.

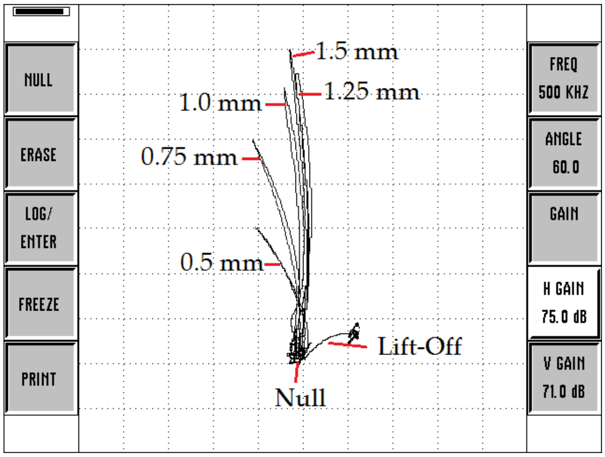

Figure 27-19 Orthogonal sensor response

Both a phase and magnitude curve can be generated. Figure 27-20 shows the phase curve and Figure 27-21 shows the magnitude curve.

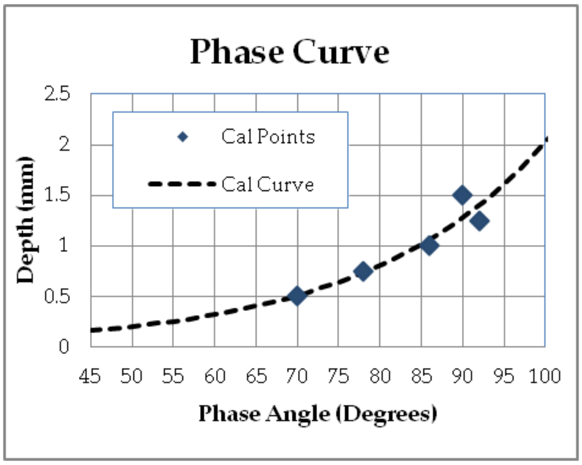

Figure 27-20 Orthogonal sensor phase curve

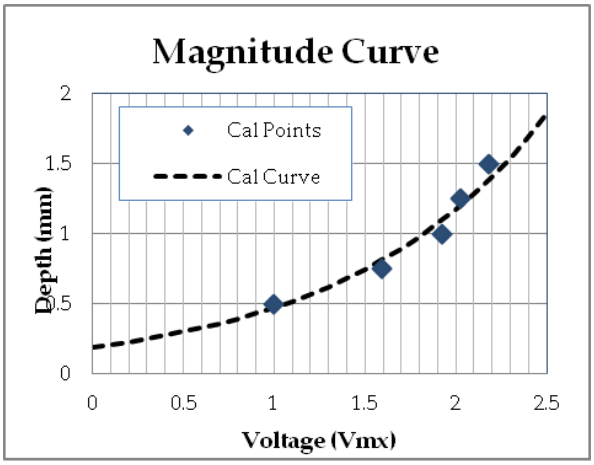

Figure 27-21 Orthogonal sensor magnitude curve

With this example, the phase curve is most accurate for shallow targets, while the magnitude curve is more accurate for deeper indications. For this example, a dual curve is used to maintain the highest accuracy for all measurements.

Note: This orthogonal sensor is optimized at 1.0 mm depth measurement in carbon steel. Different sensors would yield different curves and accuracies for each depth.